Chapter 2

Low-cost Electric Cell–Substrate Impedance Sensing System

Chapter 2

Low-cost Electric Cell–Substrate Impedance Sensing System

2.1 Outline

Biosensor is an analytical device that consists of a biological component to detect an analyte, coupled with a physical transducer to produce a measureable signal [172]. Amongst the various classes of biosensors developed so far, cell-based biosensors express promising potential in comprehending fundamental biological processes with reference to a whole cell or a group of cells [7]. Typically, the electric cell-substrate impedance sensing (ECIS) is considered for detecting any fluctuations in the microenvironment and relaying these changes to a signal transducer. ECIS relies on measuring the change in electrical impedance by applying a constant current across the active sensing area, where the cells are allowed to form a cell monolayer after cell attachment [47], [49].

Accordingly, it is known that the positively charged silver (Ag^{+}) facilitates an increase in the cell adhesion process between bulk silver and negatively charged cell membrane through a strong electrostatic interaction [173]. In the separate works, Cao *et al*.and Gao *et al*. have reported that the Ag nanoparticles incorporation into a biomaterial facilitate an increase in the cellular functions such as adhesion, proliferation and spreading. The thin film coating of silver material has shown the properties of neither genotoxic nor cytotoxic; whereas, the good cell spreading is observed over the silver thin film [174]. Hence, it can be inferred that the silver is a low-cost noble material having good anti-microbial property and biocompatibility. Therefore, in this study we have made an attempt to use silver based electrode system. To the best of our knowledge, none of the researchers so far have considered silver (Ag) as the choice of electrode for fabricating a customized and effective ECIS system. In view of the above-mentioned facts, in the present work we demonstrate development of a portable standalone ECIS system for

studying the rate of mammalian cell proliferation using low-cost circuitry. It is a compact device comprising of ECIS system with ZigBee RF module interconnected with Arduino UNO microcontroller board for establishing wireless communication network and also for establishing as 8-bit data acquisition system, which can be placed inside a CO_2 incubator in order to facilitate proper environmental condition for the biological cells. The impedance measuring devices, which are available in the market for such kind of analysis, are costly and there is a high demand on the need of portable system for point-of-care applications especially in the field of bioengineering, healthcare and environmental science. This appears as one of the major limiting factors in extensive utilization of such devices for the characterization of cell growth.

2.2 Materials and methods

2.2.1 Material

22 × 22 mm^2 cover glass (Bluestar, India) was procured and used as a substrate to fabricate the device. Mouse myoblast (C2C12) cell line was received from NCCS, Pune, India. Dulbecco's Modified Eagle Medium (DMEM) high glucose, fetal bovine serum (FBS), penicillin-streptomycin (100 µg/mL), and gelatin (cell culture tested) were received from HiMedia, India. OP07 OP-AMP IC (Analog Devices Inc., USA), 50 MHz Function Generator (Scientech Technologies Pvt Ltd, India), ICL 8038 Signal Generator IC (Intersil America Inc., US), 25 MHz-500MSa/s Digital Storage Oscilloscope (Nvis 102CT, Nvis Technologies Pvt Ltd, India), Genuino UNO (Arduino.cc, US), Computer (HP, i5 4GB RAM Windows 10 home, Singapore) and ± 9 V battery were used in performing the experiments.

2.2.2 Microelectrode design and fabrication

The glass substrate was cleaned thoroughly using standard wet chemical cleaning procedures [167] and the cleaned substrates were loaded into the thermal evaporation chamber (Hind High Vac, model smart coat 3.0A). Research grade silver metal (99.99%, Taewon Scientific Co. Ltd, South Korea) of thickness (t ≈100 nm), was deposited on the glass substrate. A maximum electrode gap of 4 mm was fabricated in order to provide sufficient gap for improved cell adhesion on the surface and to provide a proper imaging facility. The active layer's dimensions are of 1.5 mm wide and 4 mm length as shown in Figure 2.1a. The head position (9 mm dia and 14 mm height) using 1.5 ml Cliklok Micro Centrifuge (Tarsons Product Pvt Ltd, India) tube's top was cut and sealed on the top of the microelectrode fabricated glass substrate by polydimethylsiloxane (PDMS) (Dow Corning, Sylgard 184) to avoid the leakage of culture media. In our study, we used microwell culture chamber as a customized cell-culture chamber integrated with a co-planar microelectrode. Customized culture chamber was shown in Figure 2.1b.

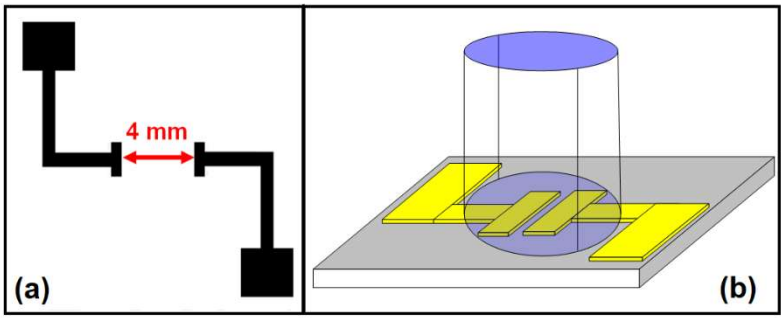

Figure 2.1: (a) Microelectrode design pattern used; (b) Customized cell-culture chamber developed.

2.2.3 Cell culture procedure

Mouse myoblast cells (C2C12) were maintained in a humidified, 5% CO_2 incubator (Galaxy 170S, Eppendorf) at 37 ºC with DMEM high glucose medium containing 10% FBS and 1% penicillin-streptomycin [175]. The microwells were coated with 2% gelatin

solution kept overnight and washed twice with phosphate buffer saline (PBS) before using [176]. The subcultured cells were grown inside the fabricated chamber. The cells were seeded at a density of 1200 cells/well, in order to visualize cellular connectivity for an optimal duration and the medium was changed prior to every observation.

2.2.4 Voltage controlled constant current source (VCCS) unit construction and testing

In principle, impedance based measurements work according to Ohm's Law which is expressed as $Z = V/I$ where, Z=impedance, V= voltage and I= current. Cells when interact and attach to the electrodes deposited on the substrate act as insulators thus contributing towards an increase in impedance [11]. The measure of opposition to the flow of electric current of cultured cells depends on various factors such as cell density covering the electrodes, morphology of the cells, type of cells and cell-cell gaps [177]. Hence, we monitored the change in dynamic behaviour of the mammalian cells under a voltage controlled constant current source (VCCS) by introducing an *in vitro* impedance analysis technique [87]. The developed system is advantageous considering the studies of dynamics of an adherent mammalian cells using miniaturized metal microelectrode. The experiments were performed in real-time, which makes it a more superior method over the conventional microscopic observations [90], [178].

Here, we used OP-AMP as integrator (or inverting amplifier) with two-voltage buffer circuit at both ends in order to avoid any loading effect. A voltage controlled constant current was supplied across the microelectrode terminals and the change in electrical potential was measured in terms of either increase or decrease in electrical impedance over the range of frequency [87], [89], [179].

Output voltage of OP-AMP is given by

$$v_{output} = -\left(v_{input} / R_1 \right) \bullet R_f \tag{2.1}$$

where, $\left(v_{input} / R_1 \right) = i_{input}$ (2.2)

R_f is variable and it is decided by the mammalian cell functioning aspects in the medium on the electrodes, while R_1 is fixed (≈ 10 kΩ) and these drives the gain of the developed circuit (ECIS setup) with a current limiting resistor (R_{limit}≈ 1 MΩ).

Gain of inverting amplifier is

$$v_{output} = -i_{input} \bullet R_f \tag{2.3}$$

Apart from this, our design does not contain any other electronic components because it suffices the requirements of measuring the activities of any biological sample. The developed ECIS system is calibrated using standard resistor values (varying from few ohms to Mega ohms) while keeping R_1 value constant with excitation frequency 2.5 kHz and excitation voltage of about 400 mV (V_{P-P}). The corresponding calibration plot using different resistor values R_1 ≈ 100 Ω, 1 kΩ, 10 kΩ & 100 kΩ is given in Figure 2.2 with R^2 ≈ 1. A optimum level of current and voltage is required in order to avoid affecting the cellular integrity [87]. Hence, the developed ECIS setup was calibrated by fixing 1 µA current and 400 mV (V_{P-P}). Hence, the developed ECIS setup showed it's functioning over the frequency range of 500 Hz to 60 kHz, to measure the behaviour of the cell without affecting the biological environment of the mammalian cells.

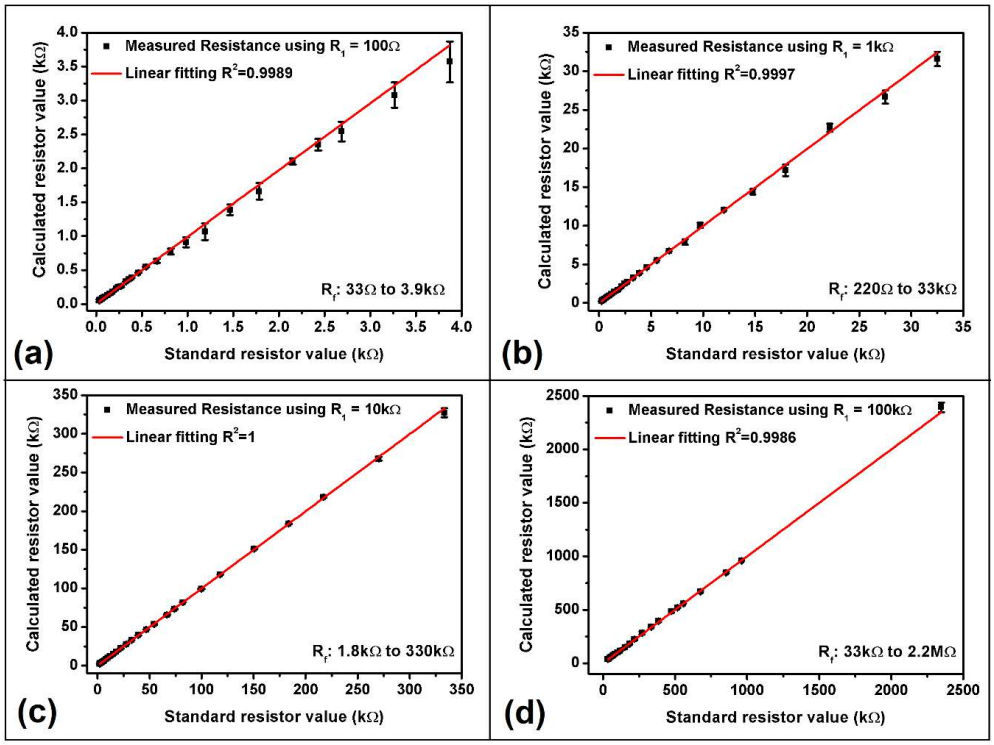

Figure 2.2: Calibration graph using different R_1 values.

The impedance (Z) is written as

$$|Z| = {V_{output}}/{i_{input}} \quad \left[|Z| \approx R_f\right] \tag{2.4}$$

The impedance of any two-terminal network can be represented as a complex quantity, which is defined in Cartesian form as

$$Z = R + jX_C \tag{2.5}$$

Where the real part is resistance R, and the imaginary part is reactance X_C. The magnitude (|Z|) and phase (ϕ) of impedance was calculated using equation 2.6 and 2.7 respectively.

$$|Z| = \sqrt{R^2 + X_C^2} \tag{2.6}$$

$$\phi = \tan^{-1}\left[X_C / R \right] \tag{2.7}$$

2.2.5 Equivalent electrical circuit Model for the cell-electrode interface

The bio-impedance analysis method of any biological medium such as organ, tissue, cells, etc. was used to characterize the changes induced by the electrical field on that medium. Hence, researchers have reported electrical modelling of the cells using the combination of resistance, capacitance, and constant phase elements to divulge the information about the cell adhesion, proliferation and differentiation [89], [109], [180], [181]. Further such devices were used as biosensors for monitoring the cell physiology in the presence of the bioactive agents (such as external stimuli, drug, etc.) [109], [182]. In addition, the cell membrane integrity and apoptosis of cells in presence of bioactive compounds have also been predicted [84], [90], [183]. Hence, by fitting the experimental data with an equivalent electrical circuit, one can calculate the theoretical relationship between the electrode-electrolyte and electrolyte-cell interface with and without the biological cells inoculated into the culture media [184]. Further, EEC model for the cell-electrode interface is discussed briefly in the **Section 2.3**.

2.2.6 Complete Electric Cell-substrate Impedance Sensing (ECIS) system

To reduce the measurement system cost, we used locally available materials to construct an impedance analyser in our laboratory. The measurement system consists of three units as follows: (1) a sinusoidal signal generation unit, where we will change the frequency and voltage needed with a current & voltage limiting circuit; (2) Inverting amplifier circuit (which will act as an Impedance analyser unit), (the pictographic image of developed ECIS system is given in Figure 2.3a and calculation procedure is given already in ECIS section); (3) Data acquisition system i.e., Digital storage oscilloscope (DSO)-

wired and Arduino Genuino UNO [both wired [27] and wireless] was used for analysing the change in electrical potential across the microelectrode. It displayed the values in Arduino Sketch software for wired communication and a pair of ZigBee RF (S1) module (one for wireless data transmission and other for receiving purpose) was used for wireless communication as shown in Figure 2.3b.

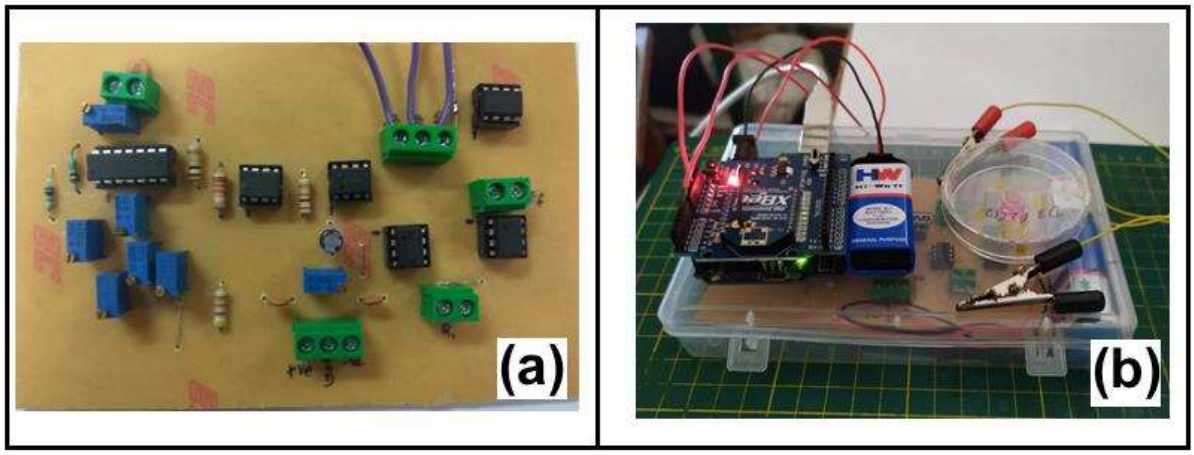

Figure 2.3: (a) Actual ECIS system, and (b) Constructed experimental (wireless) setup used with 2.5 kHz exciting frequency.

A sinusoidal signal from the signal generator was given to the feedback region of the inverting amplifier through voltage buffer and a current limiting resistor (1 MΩ) to avoid loading effect and to restrict the current flow to 1 μA. The microelectrodes were connected to the feedback region of inverting amplifier using enamelled copper wire. When C2C12 cells proliferate, a corresponding change in voltage can be observed.

Case 1: In the wired type ECIS measurement system, the change in voltage across the low-cost circuitry was simply acquired by 8-bit Arduino UNO microcontroller board and the corresponding change in impedance value was calculated and displayed in serial monitor of Arduino Sketch software.

Case 2: While for establishing a wireless communication network, ZigBee RF module was interconnected with 8-bit Arduino UNO microcontroller board and the corresponding

change in impedance value was calculated and sent to the receiving end that is displayed on the serial monitor of Arduino Sketch software. The detailed measurement process using the designed ECIS system is illustrated in Figure 2.5 as the flowchart. The ZigBee RF was used for the wireless communication protocol which is an IEEE 802.15.4-based protocol. A complete and detailed schematic representation of the developed device is shown in Figure 2.4 and a cost comparison table is provided in Table 2.1. To avoid the loading effect and (any) leakage current from the detection unit, another voltage buffer is placed in-between inverting amplifier and detection unit.

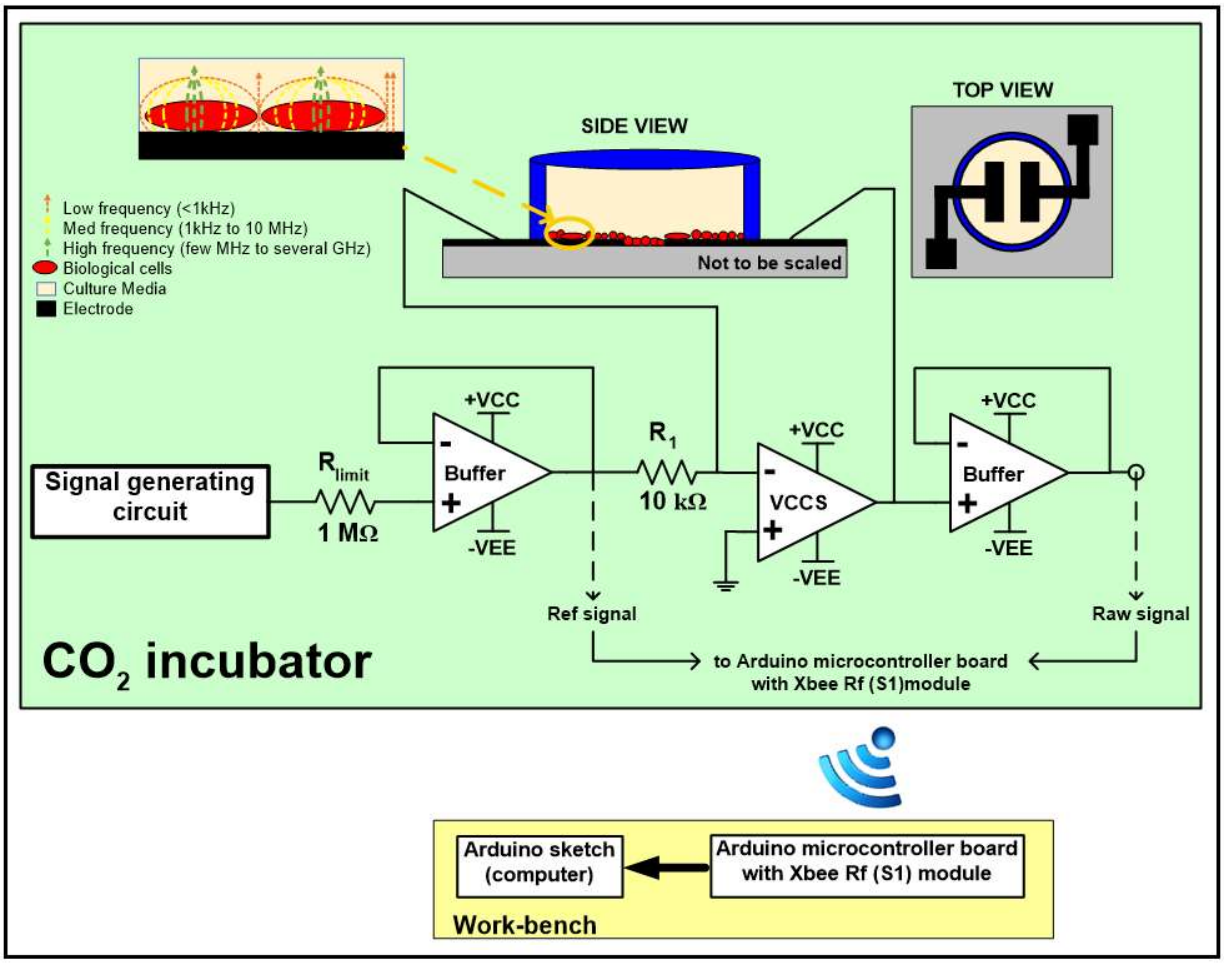

Figure 2.4: Schematic pictorial representation of the developed device.

Table 2.1: Cost comparison of the device in USD.

Commercially available instruments with its testing fixture	**DAQ based Impedance Measurement System for Low Cost and Portable Electrical Cell-Substrate Impedance Sensing [87]**	**Sensing cell-culture assays with low-cost circuitry [89]**	**Proposed ECIS System**
LCR meter (20Hz to 300 KHz/2 MHz ($4495.80 to $18769.54)	DSP lock-in amplifier - $3995.00	Circuits used (Band-Pass Filter, Bio-impedance block and Comparator circuit) + Bluetooth module + ARM Cortex-M7 microcontroller device – ($150)	Single Signal generation circuit + integrator circuit (OP-07) + components & connectors + miscellaneous charges ($50 max)
Testing fixture (excess) ($888.07 to $1610.25)	DAQ $3065.23 (starting price)	Commercial electrodes ($239.70) + Spectrum Analyser ($ 11980.00)	Arduino Genuino Uno + Wireless Shield + ZigBee (Rf) module ($101)
Connectors and micromanipulators ($695.99 & $160)	Professional software full edition (Like LabVIEW) ($5530.30)	Connectors and Testing fixture (excess) ($350.00 starting price)	Open source free software used
Total cost: $6240 to $21075	**Total cost:** $12590 (roughly)	**Total cost:** $ 12719 (roughly)	**Total cost:** $151 (roughly)

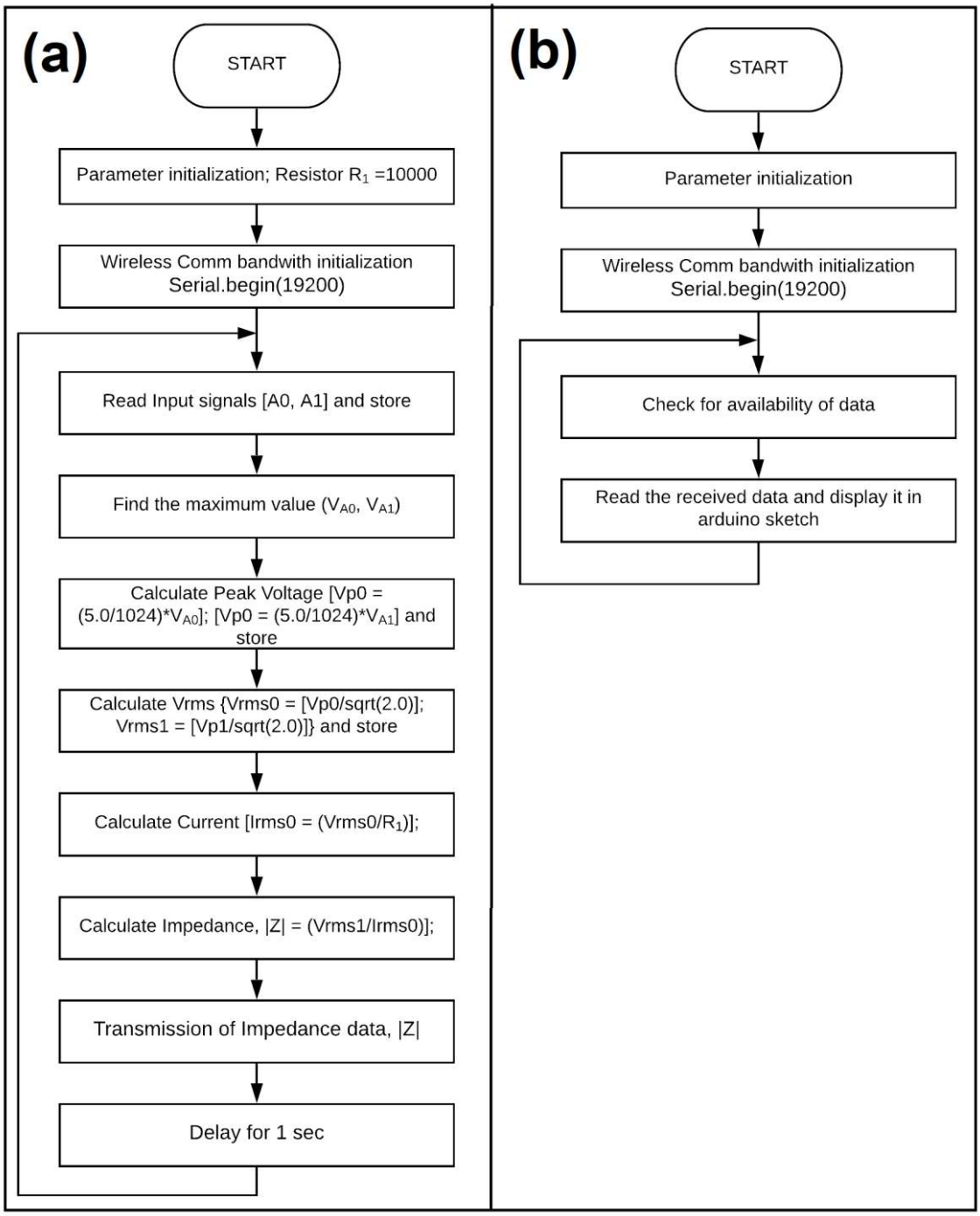

Figure 2.5: Flowchart for calculating the impedance; (a) Transmitting end, and (b) Receiving end.

2.3 Results and discussion

The basic cell growth assay was performed by seeding a lower population of C2C12 cells into the culture chamber due to its rapidly growing nature [185] in order to delay confluence and also to collect data of cellular transformations over a longer period. It can be inferred from Figure 2.6 that C2C12 cells attached, spread and proliferated on gelatin coated Ag electrodes. C2C12 cells attained their characteristic spindle shape with defined nucleus and maintained the same throughout impedance measurements; indicating that cellular adhesion and proliferation were not disturbed even during acquisition of the readings through the provided input voltage and current from the designed ECIS system. Hence, a tiny change in dynamic behaviour of the cell was observed as an increase in magnitude of impedance (as shown in Figure 2.7a).

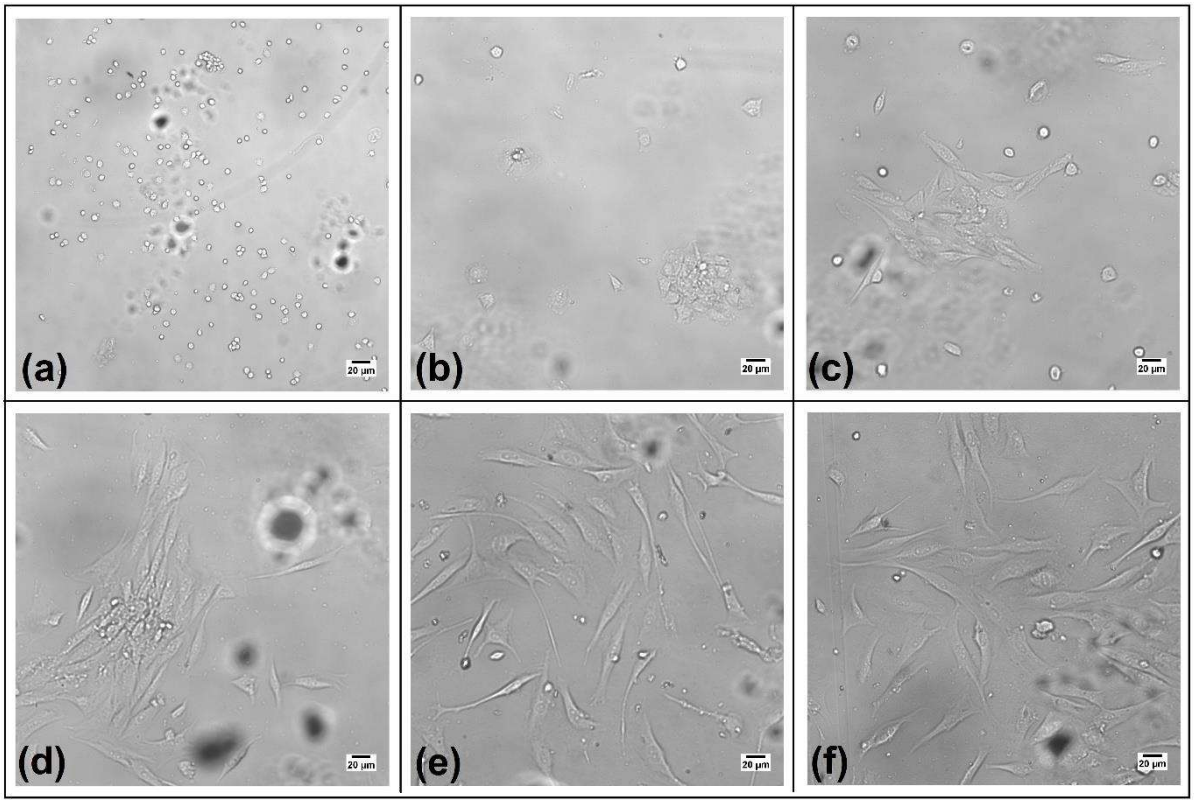

Figure 2.6: Morphological changes of C2C12 cells at various time point. (a) 3 h, (b) 6 h, (c) 18 h, (d) 32 h, (e) 48 h, and (f) 72 h; Scale bar: 20 µm.

After 3 h of culture, the shape of the cells was observed to be spheroid-like structure (as shown in Figure 2.6a); indicating that the cells were either not at all adhered or still preparing themselves to undergo through the process of adhesion (i.e., early phase of cell adhesion) on the surface of the substrate. Typically, this phenomenon (i.e., micromotion of cells) was observed as a sudden increase in magnitude of impedance (as shown in Figure 2.7a) through our developed ECIS device. The sudden increase in impedance was most likely due to the random and free-motion [81] of the biological cells suspended in the culture medium. Furthermore, the results were found in compliance with other reported papers concerning the phenomenon of the micromotion of the cells well before the adhesion on the substrate (i.e., the experimental data at 3 h) [90], [186]–[188]. Ideally, during the adhesion process, the cells suspended into the culture medium (ionic solution) adhere to the surface based on the material property by establishing a mechanical link between the cell membrane and the substrate with the help of focal adhesion transmembrane proteins i.e., integrin $\alpha v \beta 3$ and plaque proteins (paxillin, vinculin, etc.) [189].

After 6 h of culture, we observed a significant change in the cell morphology: the cells became flatten upon adhesion on the substrate, which was evidenced through the microscopic observation as represented in Figure 2.6b. Due to such changes, a noted increase in the impedance value was also observed. Further, through the normalized impedance data (as represented in Figure 2.8a), we observed that changes in the cellular morphology correspondingly influence the impedance values, as shown in Figure 2.7. In order to qualitatively evaluate our hypothesis and the impedance results, we studied the morphological changes and rate of cell proliferation in terms of increase in number (as shown in Figure 2.8b) using microscopic imaging technique.

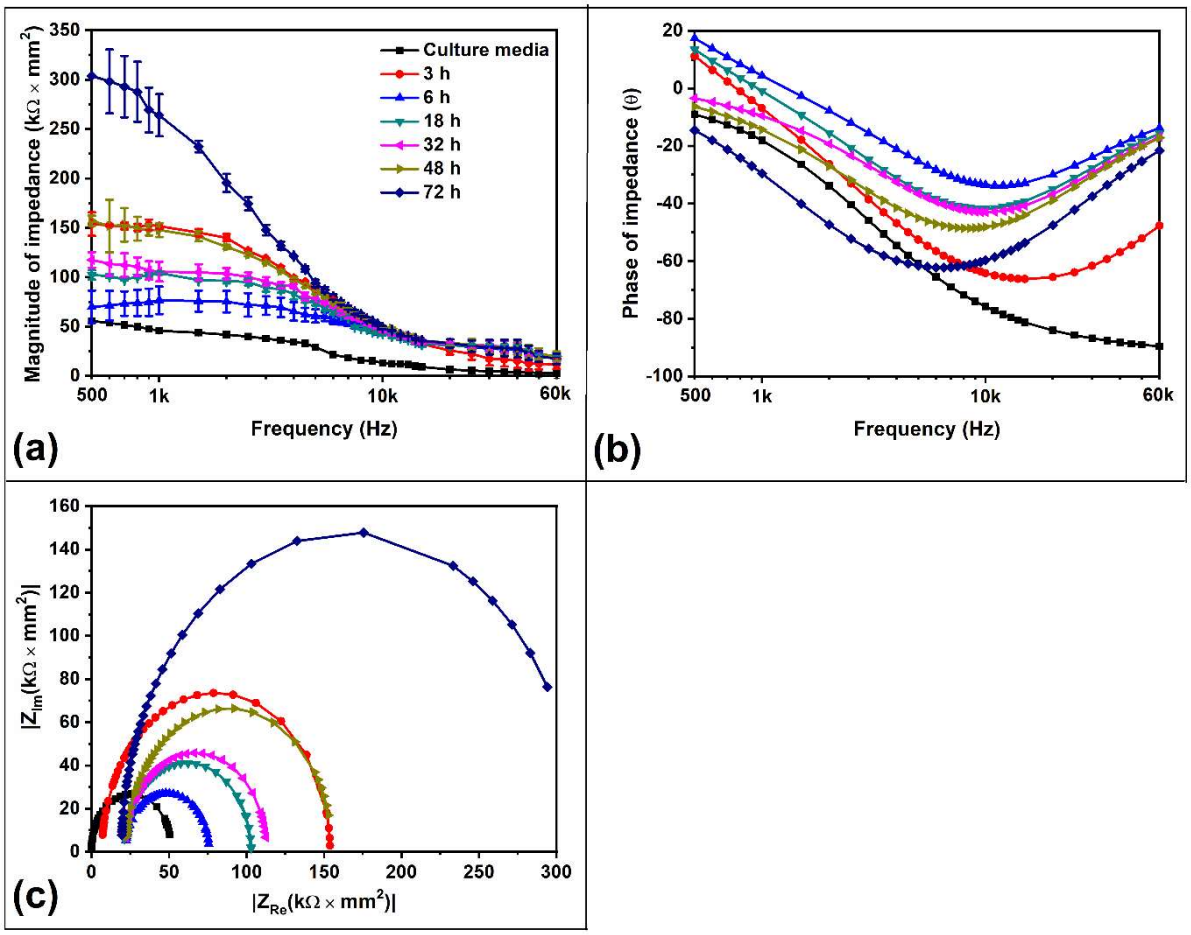

Figure 2.7: Change in cell proliferation with respect to average magnitude of impedance over the calibrated area. (a) Frequency *vs.* Magnitude (b) Frequency *vs.* Phase (c) Nyquist plot shows the change in semi-circle diameter due to the change in transfer of electrons between the metal-electrode interface resistances.

The cell number calculation was performed manually by considering 5 images and the average and SD values are given in shown in Figure 2.8b. Figure 2.6 shows the microscopic images of C2C12 cells grown on a substrate at various time points and the respective impedance values recorded as displayed in Figure 2.7. Impedance analysis of the cells was performed at various time points with modulating time gap in order to avoid disturbance in the developed biological environment. All the experiments were done in n = 5 and the average data were represented.

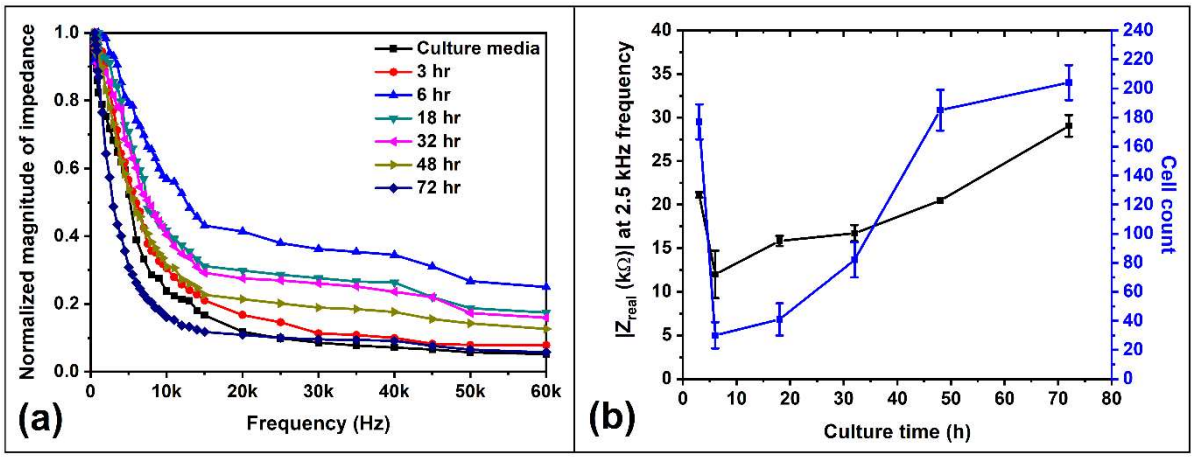

Figure 2.8: Rate of proliferation with respect to impedance (a) Normalized impedance *vs.* frequency plot, and (b) Time point *vs.* change in impedance and average cell count per image.

Biological entities are supremely heterogenic in nature that comprises of numerous non-conductive components that imparts impedance. Cells contain intracellular fluid that is enveloped with the phospholipid bilayer. Both intracellular and extracellular fluid of the cells contain ions that designates them as electrolytes [190]. The embedded transmembrane proteins within the phospholipid bilayer regulates the transport of ion and water across cellular membrane. Additionally, the cell membranes also consists of sphingolipids and cholesterol that are very poor electrical conductors at lower frequencies but significantly adds up to the impedance values [191]. Therefore, the variation in the values of impedance reflects an alteration in the cellular physiology arising due to cell spreading and attachment. Despite measuring the presence of living cells, impedance value curtails the influence of dying cells. The disintegration of the plasma membrane of the fading cells no longer serves as a barrier to the current. We observed as the cells began to interact and proliferate on the electrodes the resistance values started to surge resulting in an increased impedance; while the change in phase of impedance was directly correlated with the corresponding change in the morphology of the biological cells [192]. Thus, from the phase plot (as shown in Figure 2.7b), it was inferred that the change in

cell morphology significantly influences the experimental output. Further, we have shown the Nyquist plot (Figure 2.7c) for the cell growth at various time points, wherein we have found a noticeable change in diameter of the semi-circle that could be attributed to the change in transfer of electrons between the metal-electrode interface to the cell-electrolyte interface. This phenomenon is observed most likely due to change in the free-space in and around the metal microelectrode [193], and it also reflects the degree of homogeneity present. The deviation in the semi-circle is most likely due to the change in degree of homogeneity, conductivity and phase shift of the constant phase element (Z_{CPE}). The Z_{CPE} depends on double-layered capacitance (Q_{cell}), which is modulated by the empirical parameter '*n*'. Therefore, this could be due to change in the cell morphology during exhibition of the basic cellular functions such as cell attachment, spreading and proliferation. The cell morphology of C2C12 cell in and around the metal electrode is shown in Figure 2.9. Further, we also observed that silver metal as an electrode favoured the ECIS based measurement for a prolonged duration i.e., up to 72 h. However, due to its corrosion after 72 h, further analysis was not considered very significant.

When an excitation pulse is given to the microelectrode system, a transfer of electron from the metal surface to the solution or electrolyte (especially to the ionic carrier present in the electrolyte) takes place, which leads to development of a charged double-layer across the electrode to form electrode-electrolyte interface. The developed charged double-layered interface is directly related to a capacitance (C_{dl}) in parallel with a resistance (R_{dl}), which together represented by a constant phase element (CPE_{et}) with an empirical parameter '*n*' ($0 \leq n \leq 1$). If $n = 1$, then the system is related to an ideal capacitor; whereas, if $n = 0$, then the system is related to an ideal resistor and the impedance of CPE_{et} (Z_{CPEet}) can be calculated by an equation 2.10.

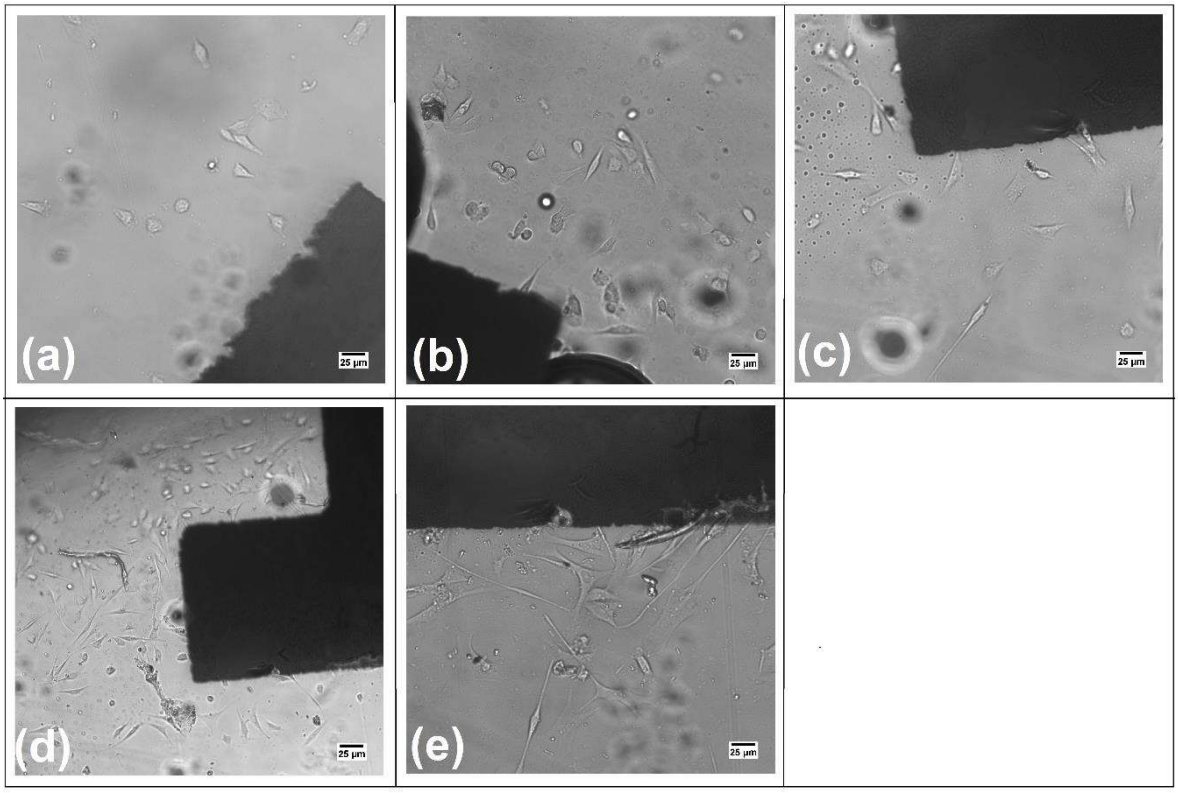

Figure 2.9: Morphology of the C2C12 cells present near the electrode (a) 6 h, (b) 18 h, (c) 36 h, (d) 48 h, and (e) 72 h; Scale bar: 20 μm.

Further, constant phase element (CPE_{et}) of electrode-electrolyte interface is used to describe several other aspects such as surface roughness of the electrodes, non-uniform current distribution, distribution of reaction rates, among other processes. While, the constant phase element (CPE_{cell}) of biological cell is used to model the cell-layer capacitance, which is due to a space charge distribution on either side of the membrane.

To fit the experimental data, researchers have used Fricke Morse model (Figure 2.10a) [194] and Cole-Cole model (Figure 2.10d) [180] to understand the physiological elements of the biological cell or tissue by correlating it with the respective passive electrical element. The resistance can be used to represent the ionic conductions, capacitance can be used to represent the polarization effects of the cell-membrane, and constant phase element was used to represent and characterize the size of cells or the tissue [180], [194].

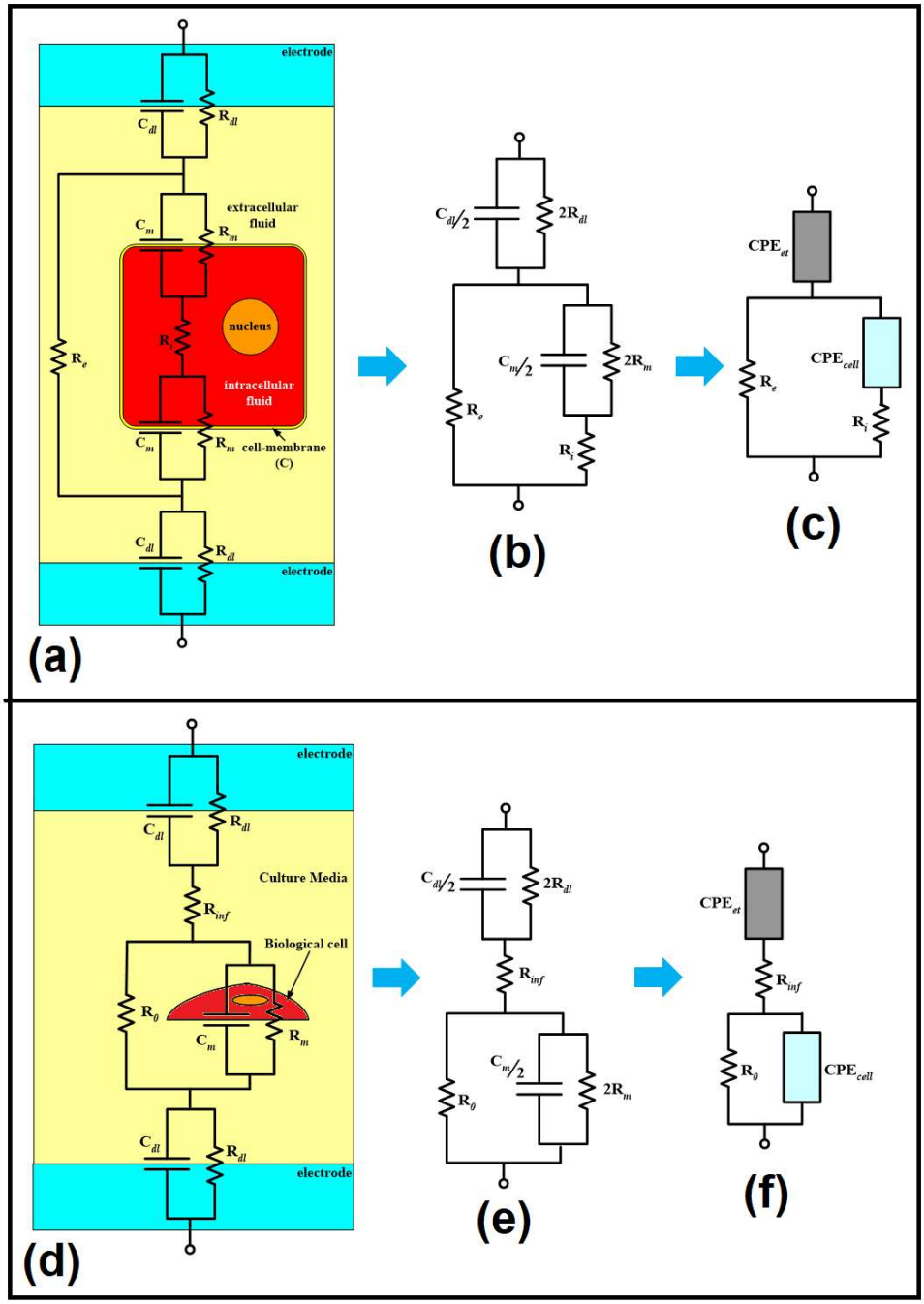

Figure 2.10: Equivalent circuit model of biological cells (a) Fricke-Morse model, (c) modified Fricke-Morse model, (d) Cole-Cole model, and (f) modified Cole-Cole model. While (b & e) are simplification step.

Therefore, any tiny quantitative change in these passive electrical parameters can divulge the functional aspects of biological cells developed as a function of its basic cellular functions. Further, it is known that the cell membrane acts as a selective ion barrier to perform various cell functions [184], [195], hence the cell membrane predominately

shows more capacitive than that of being resistance. Figure 2.10a shows the Fricke Morse equivalent electrical circuit model [44], [196], [197], for the biological cells with its simplification process and Table 2.2 shows the corresponding model parameters of the equivalent electrical model used. Generally, the biological cell can be represented by its own membrane's resistance (R_m) and capacitance (C_m) in parallel, while the inner region excluding the nucleus i.e., the cytoplasm can be represented as a resistance (R_i) and the outer region (extracellular fluid) can be represented as a resistance (R_e) or solution resistance (R_{sol}), though it has some defined electrical conductivity. Hence in the Fricke Morse model, the extracellular resistance (R_e) is kept at one arm in parallel with the intracellular resistance (R_i) and the cell-membrane (C). The cell membrane (C) consist of membrane resistance (R_m) in parallel with and membrane capacitance (C_m) in one arm. As the cell membrane (C) is nothing but a selectively permeable membrane made up of a tiny lipid bilayered film, hence it allows some of the ionic molecule/components into the cell body while it is partially permeable to some of the other organic and synthetic molecular components (such as lipid, water molecules, drug, etc.). Therefore, the cell membrane is considered as a dielectric medium or material due to its less conductivity nature. However, to represent the non-homogeneous constant present in the biological cell, the cell membrane (C) is generally represented with a constant phase element (CPE_{cell}). Thus, the Fricke Morse model was modified as shown in Figure 2.10c. Hence, the modified Fricke Morse model will provide extracellular resistance (R_e) in the one arm in parallel with the intracellular resistance (R_i), and constant phase element (CPE_{cell}) will be in another arm, while the electrode-electrolyte interfacing component CPE_{et} is kept in series. Meanwhile, the Cole-Cole electrical equivalent circuit (shown in Figure 2.10d) is used to analyse the dielectric dispersion or heterogeneity and morphological changes present in any biological medium [198]. Herein, the Cole-Cole model consists of two

resistance in order to represent both higher and lower frequency components (resistance R_{inf} & R_0) and a capacitance element to represent the cell membrane. Therefore, the higher frequency components i.e., serial resistance (R_{inf}) in one arm, while the other arm has a lower frequency component resistance (R_0) in parallel with a cell membrane (C). Later, the cell membrane (C) is being replaced by a constant phase element (CPE_{cell}) in order to represent the non-homogeneity present in the biological cells. Thus, the Cole-Cole model was modified as shown in Figure 2.10f. These CPE_{cell} is used to extract the heterogeneity and morphological change present in the biological cells of a complex biological medium. Similarly, as like in the Fricke Morse model, the electrode-electrolyte interface was represented by constant phase element (CPE_{et}) Hence, the modified Cole-Cole model will have CPE_{et} in series with the serial resistance (R_{inf}) in one arm while another arm, it will have a resistance (R_0) and CPE_{cell} in parallel.

Here in this work, the measured impedance data were fitted using Non-Linear Least Mean Square Curve Fitting Method (as shown in Figure 2.11) to analyse the non-uniformity present in the biological cells using modified Fricke Morse and Cole-Cole models. The total impedance Z($j\omega$) can be defined as in equation 2.8:

$$Z\left(j\omega\right) = Z_{\text{electrode-electrolyte interface}} + Z_{\text{Biological cell}} \tag{2.8}$$

With respect to the Fricke Morse model, the total impedance [$Z_{FM}(j\omega)$] can be defined as in equation 2.9:

$$Z_{FM}\left(j\omega\right) = \left[X_{C_{dl}} \parallel R_{dl}\right] + \left\{R_e \parallel \left[R_i + \left(X_{C_m} \parallel R_m\right)\right]\right\} \tag{2.9}$$

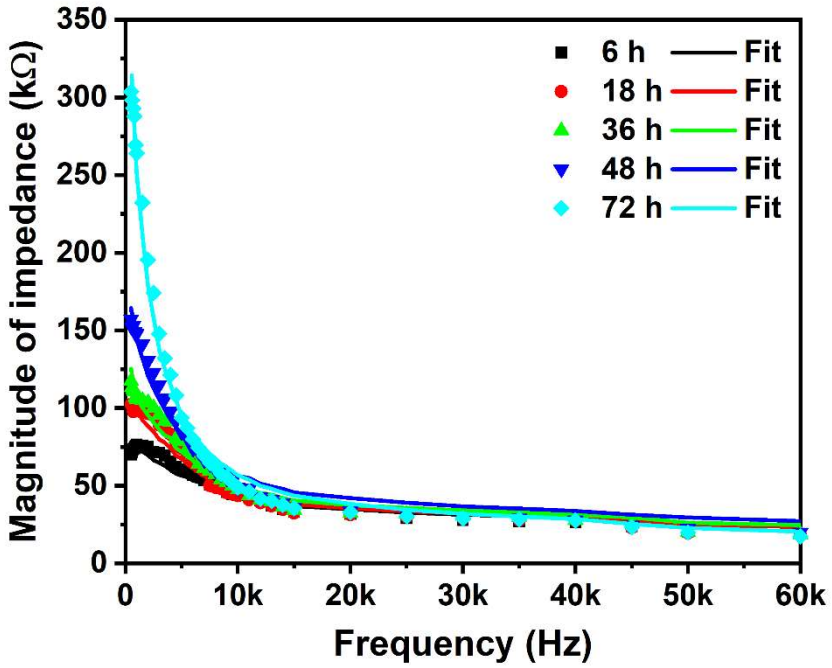

Figure 2.11: Shows the experimental data and its fitting.

Replacing the CPE of electrode-electrolyte interface (CPE_{et}) and biological cell (CPE_{cell}) in equation 2.10 & 2.11:

$$CPE_{et} = \frac{1}{(j\omega)^{\alpha_{et}} \bullet Q_{et}} \tag{2.10}$$

$$CPE_{cell} = \frac{1}{(j\omega)^{\alpha_{cell}} \bullet Q_{cell}} \tag{2.11}$$

where ω is angular frequency (rad/s),($\omega = 2\pi f$); α_{et} & α_{cell} are the CPE exponent of CPE_{et} & CPE_{cell} respectively, Q_{et} & Q_{cell} are the CPE_{et} & CPE_{cell} coefficient $\left(F/s^{(1-a_{et})}\right)$, $\left(F/s^{(1-a_{cell})}\right)$ respectively.

Hence, the total impedance of the biological cell using Fricke Morse model (equation 2.12):

$$Z_{FM}(j\omega) = \frac{1}{(j\omega)^{\alpha_{et}} \times Q_{et}} + \left[\frac{R_e \times R_i}{R_e + R_i} + \frac{R_e - \frac{R_e \times R_i}{R_e + R_i}}{1 + \left\{ j\omega \left[(R_e + R_i) \times Q_{cell} \right]^{1/\alpha_{cell}} \right\}^{\alpha_{cell}}} \right] \quad (2.12)$$

It is found that the magnitude of the total impedance offered at low frequencies is dominated by lower branch i.e., $R_e \ll |Ri + CPE_{cell}|$, hence the maximum level of current penetration in the biological cell occurs across the resistor R_e i.e., the extracellular fluid/region. On the other hand, the magnitude of the total impedance offered at the higher frequencies is dominated by $R_i \gg |CPE_{cell}|$, so the maximum level of current penetration in the medium occurs across R_e & R_i, involving both intracellular and extracellular region to approximately yields the values $[(R_e \times R_i)/(R_e + R_i)]$.

With respect to the Cole-Cole model, the total impedance [$Z_{cc}(j\omega)$] can be defined as in equation 2.13:

$$Z_{CC}(j\omega) = \left[X_{C_{dl}} \parallel R_{C_{dl}} \right] + \left\{ R_\infty + \left[X_C \parallel R_0 \right] \right\} \quad (2.13)$$

Replacing electrode-electrolyte interface and cell membrane with the corresponding CPE using equation 2.10 and 2.11, then the total impedance becomes equation 2.14 (after solving)

$$Z_{CC}(j\omega) = \frac{1}{(j\omega)^{\alpha_{et}} \times Q_{et}} + \left[R_\infty + \frac{R_0 - R_\infty}{1 + \left\{ j\omega \left[(R_0 - R_\infty) \times Q_t \right]^{1/\alpha_{cell}} \right\}^{\alpha_{cell}}} \right] \quad (2.14)$$

The magnitude of the total impedance offered at low frequencies is dominated by R_0, so the maximum level of current flow in the biological cell occurs around the extracellular region/fluid and only negligible current will pass through the biological cell due to very

high impedance/resistance R_e offer by cell-membrane. Whereas, the magnitude of the total impedance offered at higher frequencies is dominated by R_∞, so the maximum level of current in the biological medium/tissue flows inside the cell i.e., through extracellular and intracellular region/fluid R_e & R_i, to approximately yields the values $[(R_e.R_i)/(R_e+R_i)]$.

Typically, α_{et} & α_{cell} are the dimensionless exponent parameter, which reflects the dielectric loss occurred due to an alteration in the non-homogeneous constant of electrode-electrolytic interface and the cell-membrane. Therefore, when $\alpha_{et} = 1$, the CPE_{et} becomes ideal capacitor i.e., X_{Cdl} and $\alpha_{et} < 1$ is the indicator which shows the level of inhomogeneity present in the electrode-electrolyte interface. On the other hand, when $\alpha_{cell} = 1$, the CPE_t becomes ideal capacitor i.e., X_{Ccell} and $\alpha_{cell} < 1$ is the indicator which shows the level of inhomogeneity present in the dielectric medium.

Table 2.2. Analytical values through an equivalent electrical circuit model of adherent cell-electrolyte-electrode system (Fitting data derived from best of five developed microelectrode system).

FM model	α_{et}	CPE_{et}**(F)**	α_{cell}	CPE_{cell}**(F)**	R_i**(kΩ)**	R_e**(kΩ)**	R^2
6 h	8.78E-03±7.84E-06	1.13E-02±7.32E-05	0.83±0.05	9.46E-06±4.21E-06	1.21E-02±1.27E-04	15.71±3.44	0.98±1.17E-03
18 h	8.76E-03±4.45E-05	1.11E-02±4.58E-04	0.90±0.08	5.52E-06±4.18E-06	1.18E-02±5.73E-04	19.38±1.13	0.99±4.02E-03
36 h	8.78E-03±3.07E-06	1.13E-02±3.73E-05	0.92±0.03	3.88E-06±1.47E-06	1.21E-02±4.47E-05	24.53±2.93	0.99±2.45E-04
48 h	8.73E-03±5.89E-06	1.07E-02±9.87E-05	0.98±0.08	2.03E-06±1.59E-06	1.14E-02±8.74E-05	37.22±5.95	0.99±5.18E-03
72 h	8.67E-03±6.31E-05	9.82E-03±7.20E-04	0.99±0.06	1.31E-06±9.02E-07	1.05E-02±7.74E-04	45.79±10.29	0.99±2.27E-03

CC model	R_{inf} ***or*** R_{sol}**(kΩ)**	α_{et}	CPE_{et}**(F)**	R_0**(kΩ)**	α_{cell}	CPE_{cell}**(F)**	R^2
6 h	5.81E-11±3.09E-11	0.33±0.08	3.79E-02±3.22E-02	13.52±2.79	0.88±0.06	6.64E-06±3.37E-06	0.98±2.22E-03
18 h	3.61E-11±0.01E-12	0.48±0.01	1.07E-02±5.14E-04	18.48±0.02	0.84±0.01	8.58E-06±1.41E-06	0.99±3.07E-03
36 h	3.95E-11±4.75E-12	0.60±0.12	5.65E-03±1.95E-03	22.60±1.01	0.95±0.02	3.04E-06±1.07E-06	0.99±1.62E-04
48 h	3.61E-11±0.01E-12	0.68±0.03	1.44E-03±1.07E-03	33.79±2.11	0.97±0.06	1.74E-06±1.16E-06	0.99±5.39E-03
72 h	3.61E-11±0.01E-12	0.708±0.07	6.69E-04±1.96E-05	36.12±1.14	0.98±0.07	1.42E-06±9.74E-07	0.98±8.25E-03

Further, using these models it is possible to analyse the electrode-electrolyte-biological cell interfacing system. While the lower frequencies reflect interfacial effects of cell–substrate interactions, the higher frequencies reflect the morphological properties of the cell-layer formed on the electrode. Therefore, monitoring the bio-impedance spectra over a wide range of frequencies (depending upon the need) will provide us the information regarding the current state of cell functionality. Our results comply with the previously reported papers that an increase in resistance (R_e & R_0) with empirical value (α_{et} & α_{cell}) and a decrease in CPE_{cell} & CPE_{et} are primarily due to the positive rate of cell proliferation [84], [94], [109], [199] as observed from 6 h to 72 h. Thus, change in concentration of the biological cell upon the metal electrode surface was modulated with the model parameters accordingly to divulge the dynamic behaviour of any biological system.

2.4 Conclusion

This work evaluates the feasibility of a low-cost circuitry based portable, wireless ECIS system to assess the cellular dynamics of C2C12 mouse myoblasts on artificial substrates. The proposed system is working notably well with cell culture assembly designed for studying the cellular functions such as cell adhesion, spreading, migration and proliferation. The variation in physiological behaviour can be well correlated with both changes in the electrical impedance and microscopic images data as well as using an equivalent electrical model. Hence, impedance technique is capable of specifying the peak magnitude and the phase change with respect to the functional parameters of cells such as cell attachment, spreading, migration and proliferation. From the tissue engineering point of view, impedance measurements of biological entities confer a high-throughput method with temporal resolution and real-time monitoring of tissue engineered constructs in their preliminary stages regarding cell attachment, proliferation and viability.